Boundary-Layer Meteorology (2005) 114: 1–30

MICROMIXING MODELLING OF CONCENTRATION FLUCTUATIONS IN INHOMOGENEOUS TURBULENCE IN THE CONVECTIVE BOUNDARY LAYER

ASHOK K. LUHAR[1,*] and BRIAN L. SAWFORD[2]
[1]*CSIRO Atmospheric Research, PMB 1, Aspendale, Victoria 3195, Australia;* [2]*Department of Mechanical Engineering, Monash University, Clayton, Victoria 3800, Australia*

(Received in final form 7 June 2004)

Abstract. The micromixing technique, widely used in engineering calculations of mixing and chemical reaction, is extended to atmospheric boundary-layer flows. In particular, a model based on the interaction-by-exchange-with-the-conditional-mean (IECM) micromixing approach is formulated to calculate concentration fluctuation statistics for a line source and a point source in inhomogeneous and non-Gaussian turbulence in the convective boundary layer. The mixing time scale is parameterised as a linear function of time with the intercept value determined by the source size at small times. Good agreement with laboratory data for the intensity of concentration fluctuations is obtained with a value of 0.9 for the coefficient of the linear term in the time-scale parameterisation for a line source, and a value of 0.6 for a point source. Calculation of higher-order moments of the concentration field for a line source shows that non-Gaussian effects persist into the vertically well-mixed region. The cumulative distribution function predicted by the model for a point source agrees reasonably well with laboratory data, especially in the far field. In the limit of zero mixing time scale, the model reduces to a meandering plume model, thus enabling the concentration variance to be partitioned into meandering and relative components. The meandering component is shown to be more persistent for a point source than for a line source.

Keywords: Concentration moments, Concentration probability density function, IECM model, Lagrangian stochastic modelling, Skewed turbulence, Turbulent diffusion.

1. Introduction

Mixing, dispersion, and chemical reaction of trace species in the atmospheric boundary layer (ABL) are important factors in understanding and modelling many features of local, regional and global air pollution. Modelling the mean concentration field due to localised sources in the ABL is well developed in both a fundamental and a practical sense, particularly in neutral and unstable conditions where the turbulence is better characterised. However, many problems such as odour nuisance, the interaction of mixing and chemistry, the propagation of flames back to the source, or the way in which animals track a

* E-mail: ashok.luhar@csiro.au

chemical signal back to a source of food or a mate (e.g., Yamanaka et al., 2003) require a knowledge of higher-order statistics of the concentration field.

The daytime convective boundary layer (CBL) is of particular interest because under convective conditions the ground-level impact of emissions from tall stacks is greatest and the daytime boundary layer is generally more chemically active. The nature of the turbulence in the CBL is also very well understood as a result of laboratory, numerical and field studies, and there are available laboratory data for concentration statistics due to point and line sources. Although the flow is complex because it is inhomogeneous and non-Gaussian, the mean shear is relatively unimportant and can be ignored throughout most of the CBL. Thus modelling of the concentration field can be simplified by relating downwind distance x and travel time t through the Taylor transformation $x = Ut$, where U is the mean wind within the CBL.

Despite this simplification, rigorous modelling of even the concentration variance using two-point marked particle models (e.g., Borgas and Sawford, 1994; Franzese and Borgas, 2002) is still some way off, and the prospect of modelling higher-order statistics using three, four or more simultaneous particles even more distant. Recently, Luhar et al. (2000), Cassiani and Giostra (2002) and Franzese (2003) have used filtering techniques to derive plume-meandering statistics from single-particle statistics with simple parameterisation methods for relative dispersion. When coupled with a model for the in-plume concentration fluctuations (following, for example, Yee et al., 1994), this approach gives good agreement with laboratory and numerical estimates of the meandering and relative dispersion, and the ground-level intensity of concentration fluctuations. However, a major disadvantage of this approach is that the relative fluctuation intensity, used in the parameterisation of the in-plume fluctuations of concentration, must be known, but there are no appropriate measurements that can provide guidance for estimating this parameter. Also, the relative dispersion needs to be parameterised with proper asymptotic behaviours for each type of flow being considered.

Here we use an alternative approach, known as the micromixing technique, explored recently by Sawford (2004) for a line source in wind-tunnel grid turbulence. This technique is widely used in engineering calculations of mixing and chemical reaction (e.g., Fox, 1996, 1998; Subramaniam and Pope, 1998; Pope, 1998), and is extended here to ABL flows. A micromixing model is usually used to close the turbulent molecular mixing term in a transport equation for the joint probability density function (pdf) of velocity and the scalar (Fox, 1996; Pope, 1998). The usual method of implementing the micromixing technique coupled with a pdf model is to simulate the turbulent flow as independent Lagrangian fluid particles whose trajectories, in terms of velocity and position, are calculated as a stochastic process. All particles, including those released at the tracer source with the source concentration and the others with zero initial concentration, interact through micromixing

on a time scale that may be a function of the travel time. This interaction or micromixing* between particles changes the concentration of each particle with time and, therefore, dissipates concentration fluctuations.

There is a range of micromixing models for describing the evolution of concentration carried by each particle in the flow domain. Sawford (2004) used a single-particle Lagrangian stochastic model coupled with two micromixing models to represent the change of concentration along a particle trajectory due to mixing between the particle and its surroundings. The two micromixing models were: (1) the interaction of a particle with its surroundings by exchange with the local mean concentration – the IEM model (which is the simplest possible micromixing model) and (2) the interaction by exchange with the local mean concentration conditional on velocity – the IECM model. (Hence, it is clear that either the mean concentration field or the conditional mean concentration field due to the tracer source needs to be known for micromixing calculations.) Sawford (2004) focused mainly on the IECM model, because the IEM model, although easier to formulate than the IECM model, is known to induce a spurious flux which influences the concentration distribution. For example, this spurious flux causes the mean concentration field predicted by the IEM micromixing method to differ significantly from that obtained in the absence of micromixing (see Sawford, 2004). In other words, the IEM model does not fulfil the requirement that one-point statistics, such as the mean concentration, must remain unaffected by micromixing. Sawford (2004) showed that the IECM model gives remarkably good agreement with a range of different wind tunnel data for line sources as well as for a two-source configuration. In this paper we consider only the IECM approach.

Because of the simplicity of the grid turbulence, Sawford (2004) was able to obtain a number of results analytically, including expressions for the mean concentration field and the mean concentration field conditional on velocity. These analytical results were then used in the mixing calculation using a Lagrangian model, which requires a numerical solution. There are three important elements of Sawford's results that we want to emphasise here. Firstly, although he was able to derive many results analytically for grid turbulence, the key point is that in general one-point statistics such as the mean concentration and the conditional mean concentration due to a tracer source can be pre-calculated numerically from a Lagrangian marked particle model, and they remain unaltered by the micromixing (as mentioned above, this is true for the IECM model, but not for the IEM model). Secondly, Sawford showed that the mixing time scale t_m for a plume is essentially a linear function of time, with corrections very close to the source for the finite size of the source, and if it is relevant, the effect of molecular diffusion.

* The terms 'micromixing' and 'mixing' are used interchangeably in this paper.

Finally he showed that in the limit $t_m \to 0$, the IECM model reduces to a meandering plume model, and is thus physically consistent with the behaviour of plumes close to the source.

In this paper, we extend Sawford's approach to the cases of dispersion from point and line sources in the CBL. We outline the theory behind this approach in Section 2, where we discuss issues like the initial conditions, precalculation of the conditional mean and the form of the mixing time scale. Section 3 describes the numerical calculations of concentration fluctuation statistics for a line source and a point source. In Section 4, we present results for these two source types, and compare them with laboratory data. We summarise our conclusions in Section 5.

2. Theory

2.1. Lagrangian approach

We follow the now standard approach of representing the motion of independent fluid particles in a turbulent flow as a continuous Markov process in velocity-position ($\mathbf{u}$, $\mathbf{x}$) phase space. Thus we can write down stochastic differential equations representing increments in velocity and position along a fluid-particle trajectory at time t

$$du_i = a_i(\mathbf{u}, \mathbf{x}, t)\, dt + (C_0\varepsilon)^{1/2}\, d\xi_i(t), \tag{1}$$

$$dx_i = u_i\, dt. \tag{2}$$

According to Thomson's (1987) 'well-mixed' theory, the deterministic drift term $\boldsymbol{a}$ in Equation (1) is derived using specified Eulerian velocity statistics and so is different for different flows. We address the form of $\boldsymbol{a}$ for the CBL below. The so-called diffusion term in Equation (1) contains $d\xi_i(t)$, the incremental Wiener process with mean zero and variance dt (Gardiner, 1983), the rate of dissipation of turbulence kinetic energy ε, and the Lagrangian velocity structure function constant C_0. The form of this diffusion term is chosen to be consistent with Kolmogorov's theory of local isotropy (Monin and Yaglom, 1975).

In applying Equation (1) to the particular case of tracer dispersion within the CBL, we follow Luhar and Britter (1989) and subsequent refinements (Luhar et al., 1996). As indicated above, to do this we need to specify the Eulerian flow statistics characterising the flow. We assume that the turbulence is stationary, and take the mean wind to be constant throughout the boundary layer. The latter is correct for laboratory water tank simulations, where $U = 0$ and the effect of advection by the mean wind is simulated either by towing a point source through the tank (Deardorff and Willis, 1984; Weil

et al., 2002) or by transforming an instantaneous line into a continuous point using Taylor's hypothesis (Hibberd, 2000); it is, however, only approximately true in the atmosphere. We thus neglect the effect of shear-generated turbulence in the CBL, an approximation which can be justified so long as $U/w_* \leq 6$ (Willis and Deardorff, 1978), where w_* is the convective velocity scale. We are only concerned with the vertical and lateral velocity fluctuations of a particle when an instantaneous line source is transformed into a continuous point source. This is also true in the case of a real continuous point source if we ignore the streamwise diffusion compared to the mean advection provided $U/w_* \geq 1.2$. In the absence of shear-generated turbulence, these vertical and lateral velocity fluctuations are decoupled. We take the lateral (or crosswind) turbulent velocity to be Gaussian and homogeneous, but as is well-known, the vertical turbulent velocity fluctuations are strongly non-Gaussian and height dependent. Writing the Eulerian skewed probability distribution function (pdf) P_E for the vertical turbulent velocity as the sum of two Gaussian pdfs (loosely representing up-drafts and downdrafts), we can write the stochastic equation for the velocity along a particle trajectory (now using v and w to denote the lateral and vertical particle velocities respectively, and y and z to denote the corresponding positions) as

$$dv = -\left(\frac{C_0\varepsilon}{2\sigma_v^2}\right) v\,dt + (C_0\varepsilon)^{1/2}\,d\xi_v(t), \tag{3}$$

and, following Luhar and Britter (1989) and Luhar et al. (1996)

$$dw = \left[-\left(\frac{C_0\varepsilon}{2P_E}\right) Q_0 + \frac{\phi}{P_E}\right] dt + (C_0\varepsilon)^{1/2}\,d\xi_w(t), \tag{4}$$

where the random forcings $d\xi_v$ and $d\xi_w$ are uncorrelated. As in Luhar et al. (2002), we use $C_0 = 3$ and the normalised variance of the lateral turbulent velocity

$$\frac{\sigma_v^2}{w_*^2} = 0.2. \tag{5}$$

The expressions for the quantities $P_E(w,z)$, $Q_0(w,z)$ and $\phi(w,z)$ in Equation (4) are given in Appendix A. They are functions of the updraft and downdraft mean velocities, $\bar{w}_A(z)$ and $-\bar{w}_B(z)$, standard deviations, $\sigma_A(z)$ and $\sigma_B(z)$ and of the proportions of area occupied by updraft and downdraft, $A(z)$ and $B(z)$. The six unknowns A, $\bar{w}_A$, σ_A, B, $\bar{w}_B$, σ_B are determined from vertical profiles of the zeroth to fourth moments of the velocity, together with closure assumptions

$$\bar{w}_A = m\sigma_A, \tag{6}$$

$$\bar{w}_B = m\sigma_B, \tag{7}$$

with

$$m = \frac{2}{3} S_w^{1/3}, \tag{8}$$

where $S_w (= \overline{w^3}/(\overline{w^2})^{1.5})$ is the skewness of the vertical turbulent velocity (see Luhar et al., 1996). This closure ensures that the vertical turbulent velocity pdf P_E is Gaussian (with kurtosis $K_w = 3$) for $S_w = 0$. The profiles of the normalised second and third moments of the vertical turbulent velocity used are (Luhar, 2002):

$$\frac{\overline{w^2}}{w_*^2} = 1.7 \left(\frac{z}{z_i}\right)^{2/3} \left(1 - 0.9 \frac{z}{z_i}\right)^{4/3}, \tag{9}$$

$$\frac{\overline{w^3}}{w_*^3} = 1.2 \left(\frac{z}{z_i}\right) \left(1 - \frac{z}{z_i}\right)^{3/2}, \tag{10}$$

where z_i is the height (or depth) of the CBL. The Lagrangian time scale in the vertical direction is given as $T_{Lw}(z) = 2\sigma_w^2(z)/[C_0 \varepsilon(z)]$.

The profile of the dissipation rate of turbulent kinetic energy used here, which approximates the convection tank data of Deardorff and Willis (1985), is

$$\frac{\varepsilon z_i}{w_*^3} = 1.2 - 1.05 \left(\frac{z}{z_i}\right)^{1/3}. \tag{11}$$

The above parameterisation, which gives smaller values than does the one suggested by Luhar and Britter (1989) based on field experiments, is selected because we compare our model results with data from tank experiments. Because the flow in the lateral direction is assumed to be homogeneous, we use the vertically averaged value of dissipation rate $\varepsilon = \bar{\varepsilon} = 0.4 w_*^3/z_i$ in Equation (3) for the lateral component. The corresponding Lagrangian time scale is $T_{Lv} = 2\sigma_v^2/(C_0 \bar{\varepsilon})$.

The trajectory model is completed by equations for the displacement of fluid particles along a trajectory

$$dx = U\,dt, \tag{12}$$

$$dy = v\,dt, \tag{13}$$

$$dz = w\,dt. \tag{14}$$

In modelling data from very small sources in wind tunnel grid turbulence, Sawford (2004) included a white-noise molecular displacement term in these equations, but that is not necessary here because molecular diffusion is negligible for the laboratory data used in this paper.

The Lagrangian Equation (3) yields the following expression for the lateral plume variance under homogeneous conditions

$$\sigma_y^2 = 2\sigma_v^2[tT_{Lv} - T_{Lv}^2(1 - \exp(-t/T_{Lv}))]. \tag{15}$$

2.2. Micromixing model

The formulation in Section 2.1 describes how to construct particle trajectories in the CBL. To represent the change in the concentration of a fluid particle due to micromixing with its surroundings as it moves along its trajectory, we use the IECM model (Fox, 1996; Pope, 1998, 2000; Sawford, 2004). Fox's (1996) micromixing model is a linear combination of the IEM and IECM models, which in the limit of high-Reynolds number reduces to the IECM model. Pope (1998) observes that the IECM model is in accord with the independence-of-molecular-diffusivity hypothesis, and that, compared to the IEM model, it has the virtue of being local in velocity space and does not induce a spurious source term in the modelled scalar flux equation. According to the IECM model, on a mixing time scale t_m, the instantaneous concentration in the particle relaxes back to the local mean concentration conditioned on the velocity, $\langle c; \mathbf{u}(\mathbf{x}, t)\rangle$,

$$\frac{dc}{dt} = -\frac{1}{t_m}[c - \langle c; \mathbf{u}\rangle]. \tag{16}$$

Since the horizontal and vertical velocity fluctuations are decoupled, we can also decouple the horizontal and vertical terms in the expression of the conditional mean concentration (as shown later in Section 2.4).

In a traditional Lagrangian mean-field calculation (e.g., Luhar and Britter, 1989), *marked* fluid particles, which *conserve* their concentration, are released at the *source* and counted in a grid of receptor locations. Usually, each particle carries the same amount of material, and the number of particles released at any point is proportional to the source concentration at that point. One of the requirements of a micromixing model is that it should give the same one-particle statistics (e.g., the mean concentration and the mean flux) as this traditional marked particle calculation in which particles are released only at the source. As mentioned earlier, the IECM model satisfies this requirement.

In the present case, where particles undergo mixing with the given local conditional mean concentration, particles must be released uniformly across the flow domain to sample the full flow. Particles released from within the source initially carry a nonzero concentration, whereas those released outside the source carry zero initial concentration, but as a result of mixing all particles eventually carry a nonzero concentration. The number of particles

released must be such as to ensure that the number of particles initially with nonzero concentration, i.e., the particles from the source, is large enough to give reliable statistics near the source. As mixing progresses with time and more particles carry a non-zero concentration, the statistics improve. Since the source size is typically much smaller than the flow domain (of order 5 m for a stack in the CBL compared with a boundary-layer height of order 1000 m), we must release many more particles in these mixing calculations than in the traditional mean field calculation using marked particle trajectories.

In engineering applications, where the disparity between the source size and the flow domain is not so great as in the atmosphere, it is usual to carry out the trajectory calculations in parallel and so calculate the required conditional mean concentration over all trajectories at each time step and then to calculate the mixing according to Equation (16). On the other hand, for homogeneous grid turbulence, Sawford (2004) was able to calculate the conditional mean concentration analytically as a solution to the traditional marked particle problem, thus avoiding the need to carry out the trajectory calculations in parallel. Here we pre-calculate the required conditional mean concentration numerically using the traditional marked particle calculation in which particles are released only at the source. This is more efficient (requires fewer particles) than a cumbersome calculation within the trajectory model with mixing for the inhomogeneous CBL turbulence, and avoids the need for parallel trajectory calculations.

For a time step much smaller than the Lagrangian time scale, the solution to Equation (16) is (Sawford, 2004):

$$c(t) = c(t - \Delta t)\,\exp(-\Delta t/t_{\mathrm{m}}) + \langle c; \mathbf{u}\rangle[1 - \exp(-\Delta t/t_{\mathrm{m}})]. \tag{17}$$

We use Equation (17) for computing instantaneous concentration.

2.3. The time scale t_{m}

The mixing time scale, t_{m}, is an important parameter for fluctuation calculations in the micromixing model and needs to be specified. Sawford (2004) notes that t_{m} is associated with the time scale of turbulent eddies that control the growth of the instantaneous (or relative) plume and that are of similar size as the instantaneous plume. Hence,

$$t_{\mathrm{m}} \sim \left[\sigma_{\mathrm{r}}^2/\overline{u_{\mathrm{r}}^2}\right]^{1/2}, \tag{18}$$

where σ_{r} is the size (i.e., standard deviation) of the instantaneous plume and $\overline{u_{\mathrm{r}}^2}$ is the variance of the Lagrangian relative velocity fluctuations due to eddies of size comparable to the instantaneous plume. There are three

regimes of the growth of the instantaneous plume in homogeneous isotropic turbulence that are defined in terms of the travel time: the first regime for $t \ll t_s$ is dominated by the source characteristics (where $t_s = \sigma_0^{2/3}/\varepsilon^{1/3}$), and σ_r^2 is proportional to t^2 while $\overline{u_r^2}$ is constant with time; in the second regime for $t_s \ll t \ll T_L$ in the inertial subrange (where T_L is the Lagrangian integral time scale), the instantaneous plume grows according to the classical Richardson law, and σ_r^2 and $\overline{u_r^2}$ are proportional to t^3 and t, respectively; in the final regime for $t \gg T_L$, the relative dispersion approaches total (or one-particle) dispersion, and σ_r^2 is proportional to t while $\overline{u_r^2}$ is constant with time. Therefore, using Equation (18) in conjunction with the plume characteristics in the three regimes, it is clear that $t_m \sim t$ for $t \ll T_L$ and $t_m \sim t^{1/2}$ for $t \gg T_L$. As $t \to 0$, $t_m \sim [\sigma_0^2/\overline{u_r^2}]^{1/2} \sim \sigma_0^{2/3}/\varepsilon^{1/3}$. In Sawford's model for line sources in grid turbulence, a linear form

$$t_m = \frac{\sigma_0^{2/3}}{\varepsilon^{1/3}} + b_0 t \tag{19}$$

with the coefficient $b_0 = 1.2$ worked well. Such a model for t_m may prove a useful basis for empirical applications.

It is found that for a line source in the CBL, a value of $b_0 = 0.9$ describes water-tank data on scalar variance well (discussed later in Section 4.1.2). This value is lower than that for grid turbulence, indicating that the mixing in the CBL turbulence is more vigorous. For a point source in the CBL, a value of $b_0 = 0.6$ fits scalar variance data well (discussed later in Section 4.2.1). This value is lower than that for the line-source case, indicating that the mixing of a point-source plume is quicker or more efficient. This is plausible since only the vertical component of the turbulent kinetic energy causes mixing in the line-source case whereas in the point-source case the influence of both vertical and lateral components causes enhanced mixing. (We explored the use of a non-linear form for the time scale that satisfies $t_m \sim t^{1/2}$ for $t \gg T_L$, but, for the domain of the plume travel time (or downwind distance) considered here, the results obtained were not significantly different from those with the simple linear form (19).)

Some support for the different values of b_0 for the two source types mentioned above comes from the theoretical results obtained by Thomson (1997) in the inertial subrange for isotropic turbulence using an approximate Eulerian analysis. It can be deduced from his analysis, which corresponds to the IEM model, that the mixing time scale is a linear function of time and that the value of the proportionality constant b_0 does indeed depend on the source type. (The linear time dependence of the mixing time scale is also indicated by the Eulerian analysis of Csanady, 1967.) According to Thomson's analysis, the value of the constant is 4/3 for an instantaneous area source (or a continuous crosswind line source) and 4/6 for an instantaneous line source (or a continuous point source). Although these values are

consistent with the respective values of 0.9 and 0.6 used in our semi-empirical parameterisation of the mixing time scale, the latter are somewhat lower. This may partly be due to the fact that Thomson's analysis corresponds to the IEM model with t_m representing fluctuations due to both meander and in-plume perturbations, whereas in our IECM model t_m represents only the in-plume perturbations, which implies a smaller value of t_m than that in the IEM model.

In the limit $t_m = 0$, the mixing is instantaneous, that is the concentration of a particle at a location instantaneously becomes equal to the conditional concentration at that point. In this case, the fluctuations are generated solely by the variation of the conditional concentration in velocity space, and in the limit of Gaussian homogeneous turbulence, as shown by Sawford (2004), the expression for the concentration moments is the same as that obtained by the meandering plume approach (Gifford, 1959; Sawford and Stapountzis, 1986) in which concentration fluctuations are generated solely by meandering of the plume.

2.4. Conditional mean concentration

The conditional concentration required as an input in the micromixing model is a one-particle statistic and is, therefore, independent of mixing. It is calculated by releasing marked particles for a given source distribution, and calculating their trajectories using the stochastic model described above.

For a continuous line source extended along the crosswind direction and having a finite dimension or distribution in the vertical direction, we have the one-dimensional case of vertical dispersion (neglecting streamwise diffusion). It is shown in Appendix B that in this case the concentration conditional on the vertical velocity is given by

$$\langle c; w\rangle = \frac{Q_l}{UP_E(w;z)} \int_0^{z_i} P(z, w, t; z', 0) S(z')\, dz', \tag{20}$$

where Q_l is the strength of the continuous line source, $S(z')$ is the source distribution function (such that $\int_0^{z_i} S(z')\, dz' = 1$), $P(z, w, t; z', 0)$ is the forward joint pdf of particle position and velocity at time t given the initial condition $z = z'$ at $t = 0$, and the Eulerian vertical velocity pdf $P_E(w; z)$ is specified at height z. We use the one-particle Lagrangian stochastic model Equations (4) and (14) to determine the conditional concentration $\langle c; w\rangle$.

For a point source (with a finite dimension or distribution in the vertical and crosswind directions), one needs to consider dispersion in both vertical and lateral directions. Given the assumed independence of the vertical and lateral components of dispersion, the conditional concentration in this case can be written as:

$$\langle c; v, w\rangle = \frac{Q_{\mathrm{p}}}{UP_{\mathrm{E}}(w; z)P_{\mathrm{E}}(v)} \int_0^{z_i} P(z, w, t; z', 0)S(z')\ dz' \times \int_{-\infty}^{\infty} P(y, v, t; y', 0)S(y')\, dy', \tag{21}$$

where Q_{p} is the strength of the continuous point source, and the Eulerian lateral velocity pdf $P_{\mathrm{E}}(v)$ is independent of height.

We can use the model Equations (3), (4), (13) and (14) to determine the two-dimensional conditional concentration $\langle c; v, w\rangle$. However, the assumption that the turbulence in the lateral direction is Gaussian and homogeneous results in the following analytical solution for the lateral term (Sawford, in press):

$$\frac{P(y, v, t; y', 0)}{P_{\mathrm{E}}(v)} = \frac{1}{\sqrt{2\pi}\sigma_y(1-\rho_{vy}^2)^{1/2}} \exp\left[-\frac{(y - y' - \rho_{vy}v\sigma_y/\sigma_v)^2}{2\sigma_y^2(1-\rho_{vy}^2)}\right], \tag{22}$$

where the correlation $\rho_{vy}(t)$ between the particle velocity and the displacement (y) from the source location is

$$\rho_{vy}(t) = \frac{\overline{vy}}{\sigma_v\sigma_y} = \frac{1}{\sigma_v\sigma_y}\left(\frac{1}{2}\frac{d\sigma_y^2}{dt}\right) = \frac{\sigma_v}{\sigma_y} T_{\mathrm{L}v}(1 - \exp(-t/T_{\mathrm{L}v})). \tag{23}$$

For large times ($t \gg T_{\mathrm{L}v}$), Equation (23) suggests that $\overline{vy} = K_y(t)$, where $K_y(t)$ is the lateral diffusivity. The use of the analytical solution (22) instead of Equations (3) and (13) reduces the computational time by a large degree for calculating the conditional concentration.

Assuming that the source distribution is top-hat with a width of σ_0, integration of (22) over the source distribution gives

$$\frac{1}{P_{\mathrm{E}}(v)}\int_{-\infty}^{\infty} P(y, v, t; y', 0)S(y')\, dy' = \frac{1}{\sigma_0 P_{\mathrm{E}}(v)}\int_{-\sigma_0/2}^{\sigma_0/2} P(y, v, t; y', 0)\, dy' = \frac{F_y}{2\sigma_0}, \tag{24}$$

where

$$F_y = \left[\mathrm{erf}\left(\frac{\sigma_0/2 + y - \rho_{vy}v\sigma_y/\sigma_v}{\sqrt{2}\sigma_y(1-\rho_{vy}^2)^{1/2}}\right) + \mathrm{erf}\left(\frac{\sigma_0/2 - y + \rho_{vy}v\sigma_y/\sigma_v}{\sqrt{2}\sigma_y(1-\rho_{vy}^2)^{1/2}}\right)\right]. \tag{25}$$

Hence the conditional concentration due to a point source is

$$\langle c; v, w\rangle = \frac{Q_{\mathrm{p}}}{UP_{\mathrm{E}}(w; z)}\frac{F_y}{2\sigma_0}\int_0^{z_i} P(z, w, t; z', 0)S(z')\, dz'. \tag{26}$$

3. Numerical Calculations

3.1. Conditional concentration

To calculate $\langle c; w\rangle$ for a line source, we released N ($=3\times10^7$) marked particles uniformly between the source extent $z_s-\sigma_0/2$ and $z_s+\sigma_0/2$, with their initial vertical velocities randomly sampled from the skewed Eulerian distribution at the source height z_s. The skewed velocity distribution was formulated as a sum of two Gaussian distributions. We selected $\sigma_0=0.01z_i$ based on the water tank results that are used in Section 4. The particle trajectories were computed using simple finite-difference forms of the one-particle model Equations (4), (12) and (14) with the (variable) time step being $\Delta t=0.02T_{Lw}(z)$. Perfect reflection of particle vertical velocity and position was used at the top and the bottom of the CBL. The velocity and height of particles were sampled in bins of size $\Delta w=0.1w_*$ and $\Delta z=0.02z_i$. The domain of w was taken to be $-5w_*$ to $5w_*$. The mean and conditional mean concentration fields were extracted at a series of downwind distances with a spacing of $0.05z_iU/w_*$ using the following method.

If there are n_{ij} particles in the ith vertical velocity bin and jth height bin, then the integration of the joint pdf of vertical velocity and height over the source distribution is approximated numerically by

$$\int_0^{z_i} P(z,w,t;z',0)S(z')\,dz'=\frac{n_{ij}}{N\,\Delta w\,\Delta z}. \tag{27}$$

Hence the conditional concentration due to a line source is

$$\langle c;w\rangle=\frac{Q_l}{UP_E(w;z)}\int_0^{z_i}P(z,w,t;z',0)S(z')\,dz'=\frac{Q_l}{U}\frac{n_{ij}}{P_E(w;z)N\,\Delta w\,\Delta z}, \tag{28}$$

and the unconditional concentration is:

$$\langle c\rangle=\frac{Q_l}{UN\,\Delta z}\sum_i n_{ij}=\frac{Q_l n_j}{UN\,\Delta z}, \tag{29}$$

where n_j is the number of particles in the jth height bin.

Similarly, for a point source, the conditional concentration is

$$\langle c;v,w\rangle=\frac{Q_p}{U}\frac{n_{ij}}{P_E(w;z)N\,\Delta w\,\Delta z}\frac{F_y}{2\sigma_0}, \tag{30}$$

and the unconditional concentration is

$$\langle c\rangle=\frac{Q_p}{UN\Delta z}\frac{F_y}{2\sigma_0}\sum_i n_{ij}=\frac{Q_p n_j}{UN\,\Delta z}\frac{F_y}{2\sigma_0}, \tag{31}$$

where F_y is given by Equation (25). For this source, we selected $\Delta z = 0.05 z_i$, and the concentration field was extracted at a series of downwind distances with a spacing of $0.1 z_i U / w_*$.

The Eulerian vertical velocity pdf $P_{\mathrm{E}}(w; z)$ in Equations (28) and (30) was calculated for the various height bins as the sum of two Gaussian pdfs using the turbulence parameters (9) and (10) and the closure relationships (6)–(8) (see Luhar et al., 1996).

3.2. Micromixing calculation of concentration fluctuations

In the calculation of the conditional tracer concentration, the one-particle Lagrangian model Equations (4) and (14) were used for the vertical component while an analytical solution was used in the lateral direction. This pre-calculated conditional concentration field was used as an input in the calculation of the instantaneous concentration via the mixing model equation (17) coupled with the Lagrangian stochastic model.

In the one-dimensional (i.e., line source) case, N ($= 2 \times 10^6$) particles were released uniformly through the full vertical domain of the flow (i.e. between 0 and z_i) with their initial velocities randomly sampled from the skewed Eulerian distribution at their release heights. Particles that were released within the source extent $z_{\mathrm{s}} - \sigma_0/2$ and $z_{\mathrm{s}} + \sigma_0/2$ were assigned an initial concentration of $Q_{\mathrm{l}}/(U\sigma_0)$ (assuming a top-hat source distribution) while the rest were assigned zero initial concentration. Perfect reflection of particle vertical velocity and position was used at the top and the bottom of the CBL. The evolution of particle trajectories was determined using Equations (4) and (14) with the time step being $\Delta t = 0.02 T_{\mathrm{L}w}(z)$. The evolution of concentration carried by each particle was calculated using (17) with $\langle c; \mathbf{u} \rangle = \langle c; w \rangle$ given by Equation (28). In Equation (17), the local conditional concentration $\langle c; w \rangle$ given for the bin enclosing the particle position and velocity was used. The same bin sizes as in Section 3.1 were used for sampling. The instantaneous concentration field thus obtained was used to derive the concentration moments:

$$\langle c(z,t) \rangle = \frac{1}{n_z} \sum_{j=1}^{n_z} c_j(z,t), \tag{32}$$

$$\langle c'^2(z,t) \rangle = \sigma_{\mathrm{c}}^2 = \frac{1}{n_z} \sum_{j=1}^{n_z} c_j^2(z,t) - \langle c(z,t) \rangle^2, \tag{33}$$

$$\langle c'^3(z,t) \rangle = \frac{1}{n_z} \sum_{j=1}^{n_z} c_j^3(z,t) + 2\langle c(z,t) \rangle^3 - 3\langle c(z,t) \rangle \frac{1}{n_z} \sum_{j=1}^{n_z} c_j^2(z,t), \tag{34}$$

$$\langle c'^4(z,t)\rangle = \frac{1}{n_z}\sum_{j=1}^{n_z} c_j^4(z,t) - 3\langle c(z,t)\rangle^4 + 6\langle c(z,t)\rangle^2 \frac{1}{n_z}\sum_{j=1}^{n_z} c_j^2(z,t) - 4\langle c(z,t)\rangle \frac{1}{n_z}\sum_{j=1}^{n_z} c_j^3(z,t), \tag{35}$$

where n_z is the total number of particles in the height bin Δz ($\approx N\Delta z/z_i$) and $c' = c - \langle c\rangle$. The fluctuation intensity, skewness and kurtosis of concentration are determined as: $i_c = \sigma_c/\langle c\rangle$, $S_c = \langle c'^3\rangle/\sigma_c^3$ and $K_c = \langle c'^4\rangle/\sigma_c^4$, respectively.

In the two-dimensional (i.e. point source) case, N ($=5\times10^7$) particles were released uniformly and randomly through the full vertical and lateral domain of the flow (i.e. $0 \le z \le z_i$ and $-y_{\max} \le y \le y_{\max}$). The initial vertical velocities of the particles were randomly sampled from the Eulerian skewed distribution calculated at their release heights. On the other hand, the initial lateral velocities of the particles were randomly sampled from a Gaussian distribution with the variance given by Equation (5). To ensure that the plume was fully within the lateral domain, we selected $y_{\max} = 3\sigma_{y\max}$, where $\sigma_{y\max}$ is the lateral diffusion parameter calculated using Equation (15) for the maximum plume travel time simulated ($=5z_i/w_*$). Particles that were released within the source extent $z_s - \sigma_0/2$, $z_s + \sigma_0/2$, $y_s - \sigma_0/2$ and $y_s + \sigma_0/2$ were assigned an initial concentration of $Q_p/(U\sigma_0^2)$ while the rest were assigned zero initial concentration. Perfect reflection of particle vertical velocity and height was used at the top and the bottom of the CBL. In the lateral direction, periodic boundary conditions, i.e., $y = -2y_{\max} + y$ when $y > y_{\max}$ and $y = 2y_{\max} + y$ when $y < -y_{\max}$ with no change in the lateral particle velocity, were used. The evolution of particle trajectories was determined using Equations (3), (4), (13) and (14) with the time step being $\Delta t = 0.02\ \min[T_{Lw}(z), T_{Lv}]$. The evolution of concentration carried by each particle was determined using Equation (17) with $\langle c; \mathbf{u}\rangle = \langle c; v, w\rangle$ given by Equation (30). The same bin sizes for the point source as in Section 3.1 were used for sampling. The instantaneous concentration was used to derive the concentration moments using the same approach as in Equations (32)–(35), but with the concentration now a function of y also. For example the mean is given as:

$$\langle c(y,z,t)\rangle = \frac{1}{n_{yz}}\sum_{j=1}^{n_{yz}} c_j(y,z,t), \tag{36}$$

where $n_{yz}[\approx N\,\Delta z\,\Delta y/(2z_i\ y_{\max})]$ is the total number of particles in the box $\Delta y \times \Delta z$, where the bin size $\Delta y = 0.1z_i$.

As mentioned earlier, in the limit $t_m = 0$, the mixing is instantaneous, that is the instantaneous concentration $c(t)$ of a particle at a given location becomes equal to the conditional concentration at that location.

4. Model Results

4.1. Line source

In this section, we present the concentration statistics computed using the one-dimensional micromixing model for a line source and compare the results with data from laboratory water-tank experiments. We normalise all dependent and independent variables using mixed-layer similarity, with the convective velocity scale w_* and the CBL depth z_i as the scaling parameters. Thus, the nondimensional concentration due to a crosswind line source is $C = cUz_i/Q_l$, where c is the dimensional concentration. This concentration is equivalent to the scaled crosswind-integrated concentration due to a point source $C^y(= c^y Uz_i/Q_p)$, where $c^y = \int_{-\infty}^{\infty} c\, dy$ is the dimensional crosswind-integrated concentration.

The plume travel time (t) since its release can be transformed into equivalent dimensionless distance (X) or dimensionless time (T) for the CBL through

$$X = T = \frac{w_*}{z_i} t = \frac{w_*}{z_i} \frac{x}{U}. \tag{37}$$

4.1.1. *Model Consistency Test*

A properly formulated IECM model should fulfil the requirement that the micromixing governed by Equation (16) does not affect the mean concentration field. To check that this is indeed the case, we consider a line source release at the dimensionless height $z_s/z_i = 0.25$, and compare the mean concentration $\langle c(z,t)\rangle$ computed using Equation (32) via the micromixing model with that by Equation (29) involving the marked-particle method; they should be the same. Figure 1a and b shows contours of the dimensionless mean concentration $\langle C\rangle(= \langle c\rangle Uz_i/Q_l)$ obtained using the two respective models. It can be seen that both contour plots are virtually the same, indicating a consistent micromixing model formulation. Any differences between them arise due to numerical errors and differences in the number of particles released.

Figure 1c and d presents the dimensionless mean crosswind-integrated concentration ($\langle C^y\rangle$) contours obtained by Willis and Deardorff (1978) (for $z_s/z_i = 0.24$) and Hibberd (2000) (for $z_s/z_i = 0.25$) using a heated convection tank and a saline convection tank, respectively. In both these experiments, results from an instantaneous line source were transformed into those from a continuous point using Taylor's translation hypothesis. The model results in Figures 1a and b agree with the observed dispersion patterns, showing that the concentration maximum descends to the ground and then lifts off; however, the latter feature is not as pronounced in the model results as in the

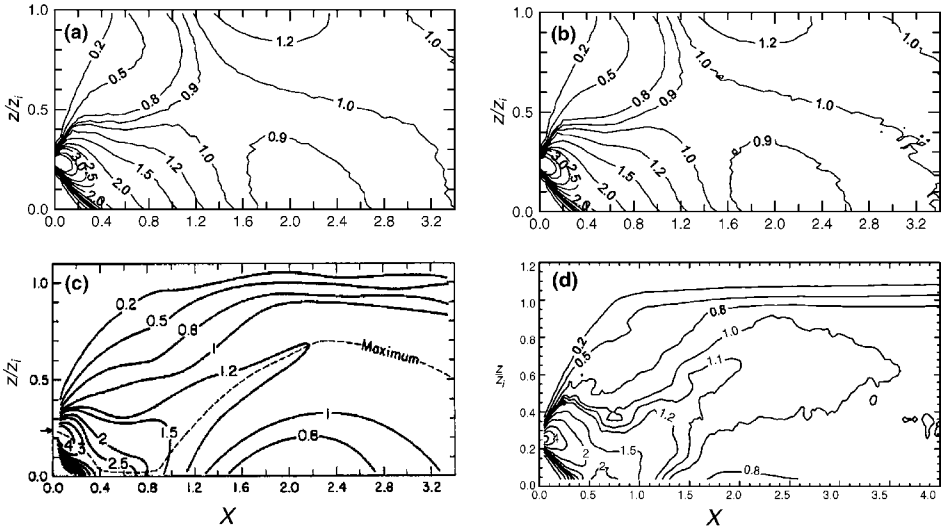

Figure 1. Contours of the dimensionless concentration due to a crosswind line source situated at the dimensional height $z_s/z_i = 0.25$ predicted by (a) the micromixing model, and (b) the marked-particle model. The equivalent contours of the dimensionless crosswind-integrated concentration due to a point-source measured by (c) Willis and Deardorff (1978), and (d) Hibberd (2000) in their water-tank experiments.

tank results. Subsequently, for about $X > 3$, the plume becomes almost well mixed through the depth of the boundary layer. The two laboratory datasets compare well, and the main difference between them is that the maximum ground-level concentration in Figure 1d is about 20% lower than in Figure 1c, and is closer to the model value. The results showing plume descent close to the source and the subsequent lift-off, now well known, are caused by the large-scale inhomogeneous and skewed convective turbulence within the CBL, and cannot be satisfactorily described by standard diffusion models (e.g., the first-order gradient transfer model or the Gaussian plume model).

4.1.2. *Concentration Fluctuation Intensity*

Our micromixing model is designed for concentration fluctuation calculations, and one measure of fluctuations is the concentration fluctuation intensity. Hibberd (2000) conducted a series of laboratory experiments with passive releases at four different heights, namely $z_s/z_i = 0.08$, 0.25, 0.42 and 0.80, and determined the variation of the fluctuation intensity ($i_c = \sigma_c/\langle c^y \rangle$) of the crosswind-integrated concentration, which, as mentioned earlier, is equivalent to the fluctuation intensity due to a crosswind line source.

The diamonds in Figures 2a–d represent the variation of the near-surface $(z/z_i = 0.05)i_c$ with X measured in the laboratory experiments for the four

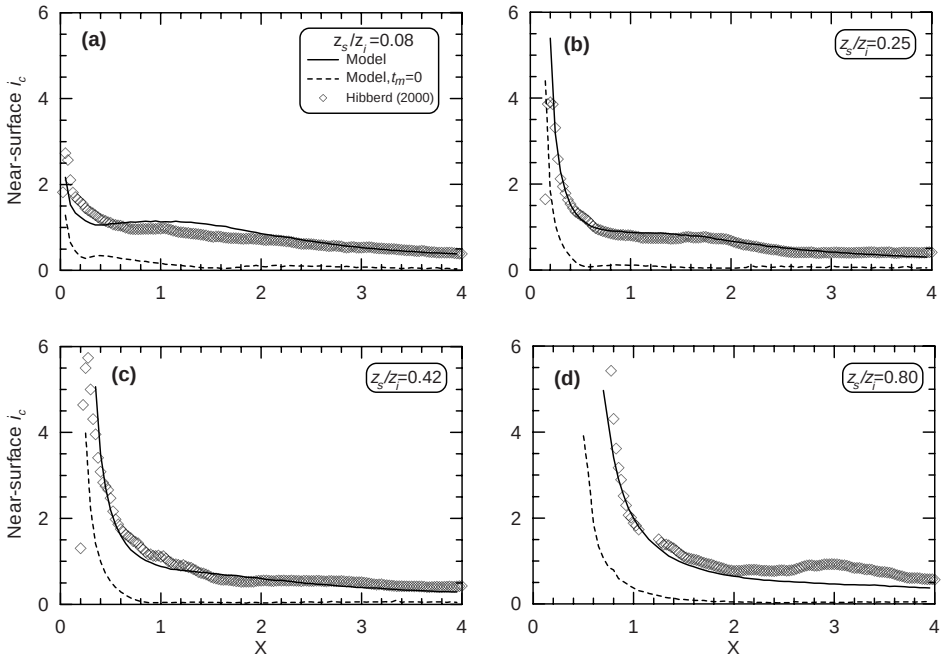

Figure 2. Variation of the near-surface ($z/z_i = 0.05$) concentration fluctuation intensity (i_c) with dimensionless distance (X) for the one-dimensional vertical dispersion case. The diamonds are the water-tank data of Hibberd (2000) for the tracer release heights (z_s/z_i) of (a) 0.08, (b) 0.25, (c) 0.42, and (d) 0.80, whereas the solid lines are the corresponding micromixing model results. The dashed lines are the micromixing model results in the limit $t_m = 0$.

source heights. Except for the one or two points closest to the source in Figures 2a–c, the observed i_c decays with distance as the plume grows. The experimental data points closest to the source showing a decreasing i_c with decreasing X are probably not representative of the actual behaviour because the sample size for these points may not be large enough due to the fact that the plume rarely reaches the ground so close to the source location. As the source height increases, the fluctuation intensity close to the source becomes larger because the ground increasingly experiences more of the plume edges rather than the inner plume.

The solid lines in Figures 2a–d are the micromixing model results obtained using t_m given by Equation (19) (with $b_0 = 0.9$) whereas the dashed lines are the model curves for $t_m = 0$. The difference between the two types of model curves is that in the former the concentration fluctuations are generated by the meandering of the plume as well as by in-plume fluctuations, whereas in the latter they are generated solely by the meandering. With increasing distance downstream the plume undergoes progressively less meandering and in-plume fluctuations contribute increasingly to the total fluctuation intensity.

The solid curves agree very well with the data, which is not too surprising because the value of b_0 has been selected to fit the data. However, what is interesting is that the simple linear form for t_m, with a single b_0 value, describes the data well for all source heights. On the other hand, this observation may not be true in general. For example, in cases where there is significant mean wind shear (ignored here in the case of CBL) the mixing time scale may have spatial dependence as well. The dashed lines indicate that there are almost no fluctuations due to meandering for $X > 1.5$.

Figures 3a–d present contour plots of the concentration fluctuation intensity measured in the laboratory experiments for the four source heights, whereas Figures 3e–h are the corresponding model plots. It can be seen that, at a given downwind distance close to the source, the observed i_c becomes larger towards the plume edges and approaches a minimum at the plume centreline. The distribution of i_c is almost uniform across the bulk of the boundary layer for about $X > 2.5$. Although the model contours are similar to the observed ones, a couple of differences are prominent. First, at heights close to the top of the boundary layer ($z/z_i \approx 1$), the vertical gradients of the observed and modelled i_c are opposite for about $0.7 < X < 2.5$ for the lowest three sources heights. This is most probably due to the fact that in the model both the top and the bottom of the boundary layer are treated as 'hard' boundaries with perfect particle reflection there, whereas in the laboratory tank the top is a 'soft' boundary with enhanced plume fluctuations due to undulations in the boundary-layer top. The porous boundary-condition scheme suggested by Thomson et al. (1997) may be more appropriate than that used here. Second, for the source height $z_s/z_i = 0.8$ in the tank experiments, there is a well-defined local minimum at the top of the CBL and a local maximum just below it for $X \approx 0.7$ (Figure 3d). Also, there is a weak local maximum represented by a slanted contour of value 2 below the release height. These features are not simulated by the model because in the tank some tracer was trapped in the weakly dispersive entrainment zone with less fluctuations while those parts of the plume that were not trapped follow the behaviour represented by the model. The model does not explicitly account for the entrainment zone.

4.1.3. *Higher-Order Moments*

Figures 4a and b present contours of the skewness (S_c) and kurtosis (K_c), respectively, of the concentration distribution computed from the model. There are no data to compare these plots with. It can be seen that the skewness is always positive, and the kurtosis value is always greater than the Gaussian value of 3. This implies that the pdf of concentration at a particular point has a tail towards the higher values of concentration, and is more peaked than the Gaussian distribution. In the region close to the source where the influence of the boundaries on the plume is minimal (about $X < 1$),

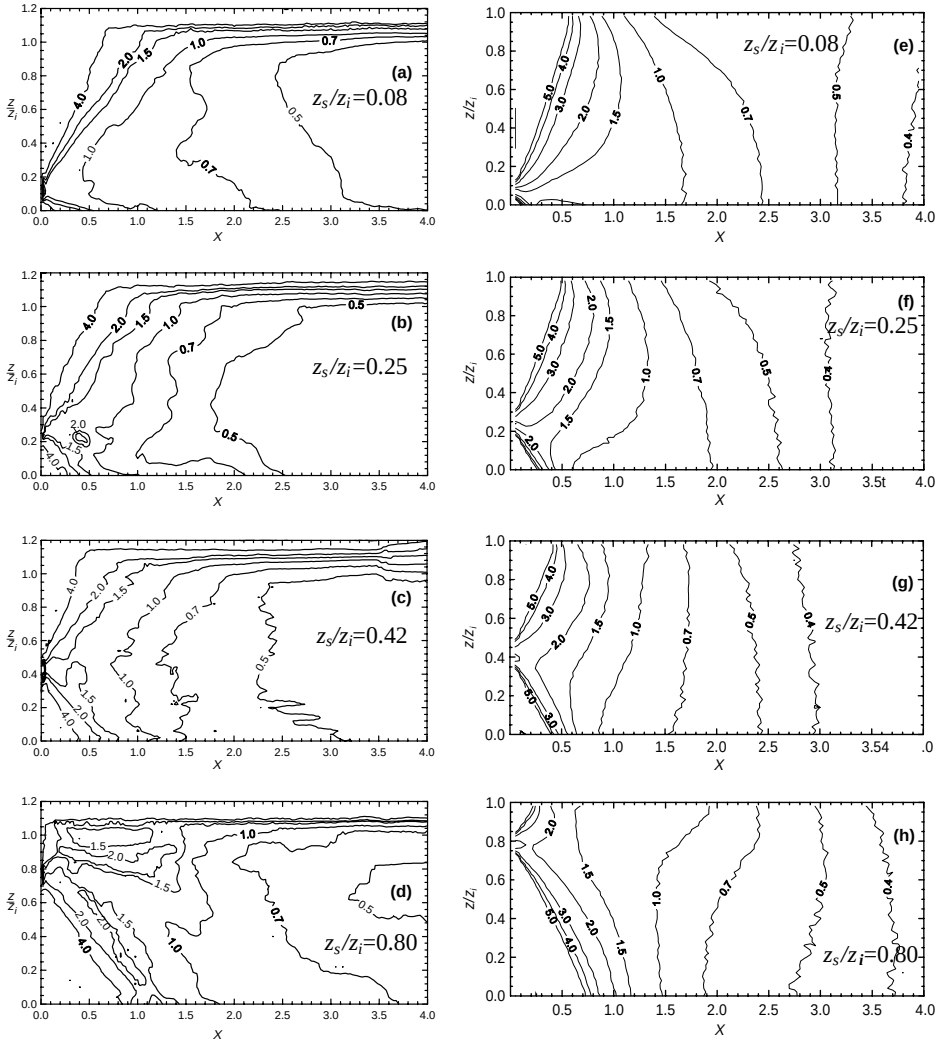

Figure 3. Contours of the concentration fluctuation intensity for the one-dimensional vertical dispersion case for tracer release heights (z_s/z_i) of (a) 0.08, (b) 0.25, (c) 0.42, and (d) 0.80, obtained by Hibberd (2000) in water-tank experiments. The contour plots e–h are the corresponding micromixing model results.

both the skewness and kurtosis values are greater in the plume edges than in the inner parts of the plume, suggesting that the concentration pdf at the plume edges has a longer tail and is more peaked (i.e., fluctuations are more intermittent). In the region where the plume is nearly well mixed in the vertical (about $X > 3$), $S_c \approx 3$ and $K_c \approx 18$. The S_c and K_c values in Figure 4 are high, and arise because the pdfs (not shown here) have 'fat' tails that almost follow a power-law relationship. However, we do not have any data

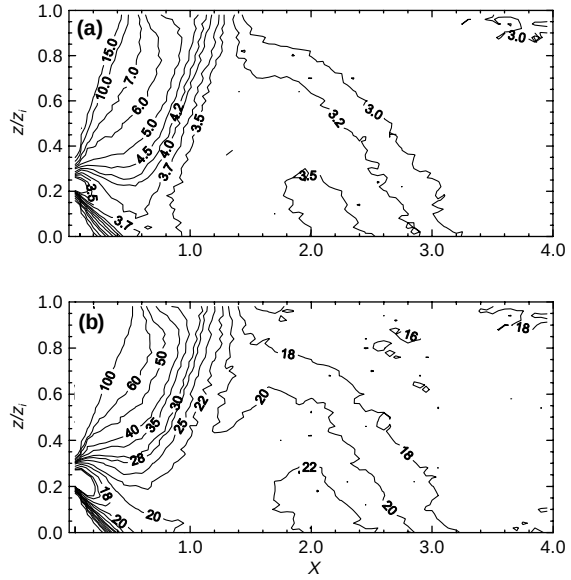

Figure 4. Contours of the (a) skewness and (b) kurtosis for the one-dimensional vertical dispersion case for the tracer release height (z_s/z_i) of 0.25 predicted by the micromixing model.

with which to compare these higher-order model moments. We might have expected mixing to produce statistics closer to Gaussian and at this stage it is not clear whether these strong non-Gaussian effects are real or an artefact of the IECM mixing model.

4.2. Point source

In this section, we present results from the two-dimensional mixing model for a point source.

4.2.1. *Concentration Fluctuation Intensity*

We compare the concentration fluctuation intensity computed using the model with the data of Deardorff and Willis (1984) and Weil et al. (2002) who conducted experiments on concentration fluctuations from buoyant and non-buoyant point sources using water tanks heated from the bottom. We only considered the data from their non-buoyant source experiments because our model is applicable only to passive releases. In both experiments, the effect of advection by the mean wind was simulated by towing the point source through the tank. In the former, the source height $z_s = 0.13z_i$ and the nondimensional initial momentum flux $F_{m^*} = 0.001$, whereas in the latter $z_s = 0.15z_i$ and $F_{m^*} = 0.004$. There was not much difference between the

arrangements of the two experiments, and we simulated them using a single model run with $\sigma_0 = 0.01 z_i$. To approximately account for the initial momentum effect, we assumed (as in Luhar et al., 2000) that the initial momentum only causes an increase in the near-source mean plume height without affecting the diffusion around it. Therefore, the virtual source height, estimated to be $z_s \approx 0.22 z_i$, to represent the momentum effects, was used in the model calculations instead of the physical source height.

Figure 5 compares the downwind variation of the near-surface ($z/z_i = 0.08$) i_c obtained by the model with the data of Deardorff and Willis (1984). The measurements denoted by open triangles represent an average over $|y| < 0.5\sigma_y$ and those denoted by open circles represent an average over $0.5\sigma_y < |y| < \sigma_y$. The solid and the dashed lines are the corresponding model predictions (with $b_0 = 0.6$ in Equation (19)), which show that the selected form of the mixing time scale leads to good agreement with the data. The noise in the model curves is largely statistical, and would reduce if an even higher number of particles was released. The model results suggest that i_c is somewhat lower in the inner region of the plume, an expected behaviour not clearly discernible in the data. Also plotted as solid squares in Figure 5 are the centreline ($y = 0$) fluctuation intensity data of Weil et al. (2002) near the surface ($z/z_i = 0.05$). The model curve for $|y| < 0.5\sigma_y$ is in good agreement with the Weil et al. data, with a slight overprediction for $X \geq 3$. (The model curve for $y = 0$, not shown here, is little different from that for $|y| < 0.5\sigma_y$.) The dashed-dot line in Figure 5 is the model centreline i_c in the limit $t_m = 0$,

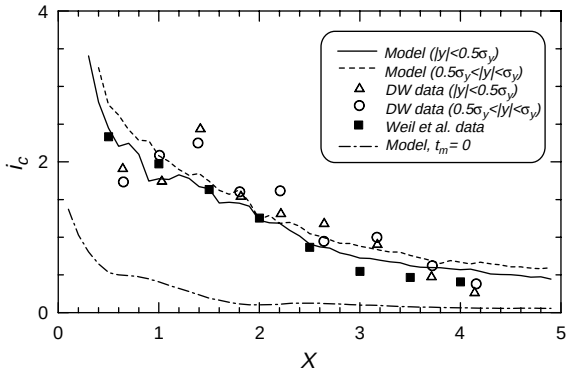

Figure 5. Variation of the near-surface concentration fluctuation intensity (i_c) with the dimensionless distance X for the (two-dimensional) point-source case for $z_s/z_i = 0.22$. The measurements of Deardorff and Willis (1984) averaged over $|y| < 0.5\sigma_y$ and $0.5\sigma_y < |y| < \sigma_y$ are represented by triangles and circles, respectively. The lines are the corresponding micromixing model predictions. The water tank data of Weil et al. (2002) taken at the plume centreline ($y = 0$) are shown as solid squares. The dashed-dot line is the model centreline i_c in the limit $t_m = 0$, which corresponds to fluctuations due to meander only.

which corresponds to fluctuation due to plume meander only. It is clear that plume meandering is negligible for $X > 3$.

Figure 6 presents model contours of the fluctuation intensity along the plume centreline. Although the contours are somewhat noisy, the trends are clear. As in the line source case shown in Figure 3f for a source at similar height, the fluctuation intensity becomes larger towards the plume edges and approaches a minimum at the plume centreline. However, i_c is roughly twice a large as that in the case of a line source.

The variation of the near-surface i_c along the crosswind (y) direction at dimensionless distances $X = 0.5$, 1.5, 2.5 and 3.5 is presented in Figure 7. The circles are the data of Weil et al. (2002) and the lines are the model results. It is apparent that overall the model simulates both the width and the magnitude of the crosswind distribution of the observed i_c very well. The fluctuation

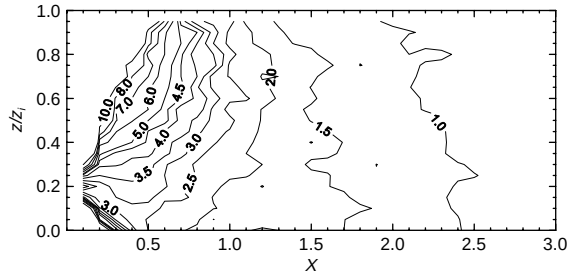

Figure 6. Contours of the concentration fluctuation intensity (i_c) along plume centreline ($y = 0$) predicted by the micromixing model for the point-source case for $z_s/z_i = 0.22$.

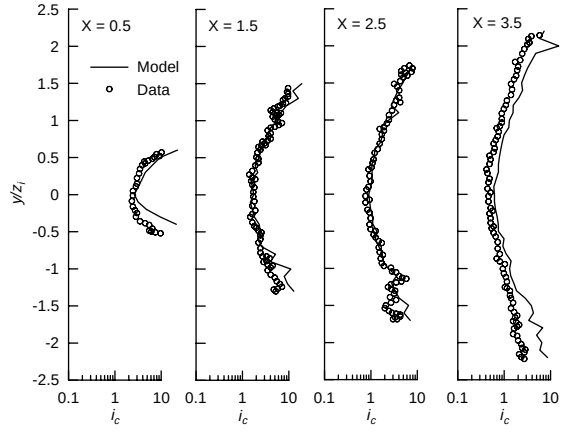

Figure 7. Crosswind profiles of the concentration fluctuation intensity (i_c) near the surface ($z/z_i = 0.05$) as a function of nondimensional distance (X) for the point-source case. The open circles are the laboratory data of Weil et al. (2002) and the solid lines are the model predictions.

intensity increases in the plume edges and decreases with X. At $X = 3.5$, the model intensities are somewhat higher than the data, and at $X = 0.5$ the width of the i_c variation predicted by the model is slightly narrower than the observations.

4.2.2. *Cumulative Distribution Function*

In Figure 8, the shape of the cumulative distribution function (CDF) of the normalised concentration $(c - \langle c \rangle)/\sigma_c$ at $y/z_i = 0$, $X = 4$ and $z/z_i = 0.5$ predicted by the micromixing model (solid line) closely resembles the laboratory data (open circles) reported by Weil et al. (2002), including the extreme tail of the concentration distribution. These researchers show that at this X value, where the mean plume is nearly well mixed in the vertical, the laboratory CDF does not vary much with height, a result also indicated by the model predictions (not shown here).

The dashed line in Figure 8 shows the centreline CDF predicted by the model at $X = 0.5$ and $z/z_i = 0.4$ whereas the open triangles are data extracted from a narrow band of observed centreline values corresponding to the same distance and $z/z_i = 0.075 - 0.5$ presented by Weil et al. Although the qualitative shape of the observed CDF is captured reasonably well by the model, there are significant differences. For example, the model does not appear to

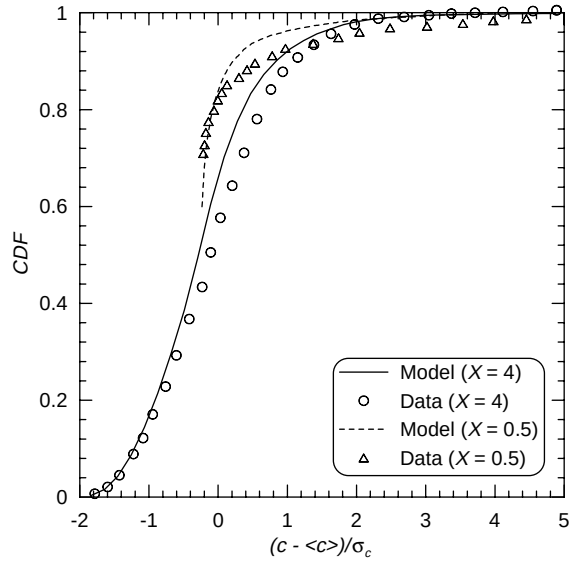

Figure 8. Cumulative distribution function (CDF) of the normalised concentration at the plume centreline ($y = 0$) predicted by the micromixing model (for source height $z_s = 0.22z_i$) at $X = 4$ and $z/z_i = 0.5$ (solid line), and at $X = 0.5$ and $z/z_i = 0.4$ (dashed line). The open circles and open triangles are the laboratory data of Weil et al. (2002) at $X = 4$ and $X = 0.5$, respectively, at similar heights as the model results (see Section 4.2.2 for more details).

capture adequately the observed long-tail of the concentration distribution. At $(c - \langle c \rangle)/\sigma_c = 3$, the model CDF value is about 0.99, whereas the observed CDF value is about 0.96. This results in a factor of 4 difference in the probability of occurrence of the $c = \langle c \rangle + 3\sigma_c$ value.

Weil et al. (2002) observe that overall the gamma CDF is a reasonable fit to the measured CDFs, and is a significantly better fit than the clipped-normal CDF when $i_c \geq 1$ (i.e., in the near field). For $i_c \approx 0.4$ (i.e., in the far field), the clipped-normal CDF is in better agreement with the data, but the gamma CDF is a slightly better fit in the tails.

4.2.3. *Lateral Plume Dispersion*

In our model, we have assumed that the turbulence in the lateral direction is homogeneous and Gaussian and does not vary with height. Sawford (2004) shows that for such a turbulent flow, the standard deviation of the plume meander implied by the IECM micromixing model is

$$\sigma_{y\mathrm{m}} = \sigma_y \rho_{vy}, \tag{38}$$

where the mean plume spread σ_y due to turbulence is given by Equation (15), and ρ_{vy} is given by Equation (23). The relative standard deviation is

$$\sigma_{yr} = (\sigma_0^2 + \sigma_y^2 - \sigma_{y\mathrm{m}}^2)^{1/2} = [\sigma_0^2 + \sigma_y^2(1 - \rho_{vy}^2)]^{1/2}. \tag{39}$$

The solid line in Figure 9a represents the variation of the normalised total plume spread in the lateral direction, $(\sigma_0^2 + \sigma_y^2)^{1/2}/z_i$, where the velocity variance (5) and the depth-averaged kinetic energy dissipation rate ($\bar{\varepsilon} = 0.4 w_*^3/z_i$) were used to calculate σ_y. The laboratory data of Willis and Deardorff (1976, 1978, 1981) and the large-eddy simulation (LES) results of Nieuwstadt (1992) for various source heights are also shown. Since the lateral turbulence is assumed to be horizontally and vertically homogeneous, the analytical variation does not depend on the source height; however, it represents the overall data points well.

The variation of the normalised lateral relative spread $\sigma_{y\mathrm{r}}/z_i$ calculated using Equation (39) with ρ_{vy} given by Equation (23) is shown in Figure 9b as a solid line, which is supported by the LES results. The dashed line represents the interpolative parameterisation of $\sigma_{y\mathrm{r}}/z_i$ developed by Luhar et al. (2000) (their Equation (22)) based on the relative dispersion theory. It is remarkable that the present curve based on the simple analytical result obtained within the micromixing framework agrees so well with the dashed line.

The variation of the normalised meander spread, $\sigma_{y\mathrm{m}}/z_i$, determined using Equation (38) is shown as a solid line in Figure 9c, together with the LES results. The meander spread calculated by Luhar et al. (2000) is also shown as a dashed line. It is evident that the LES results show a higher peak spread. At

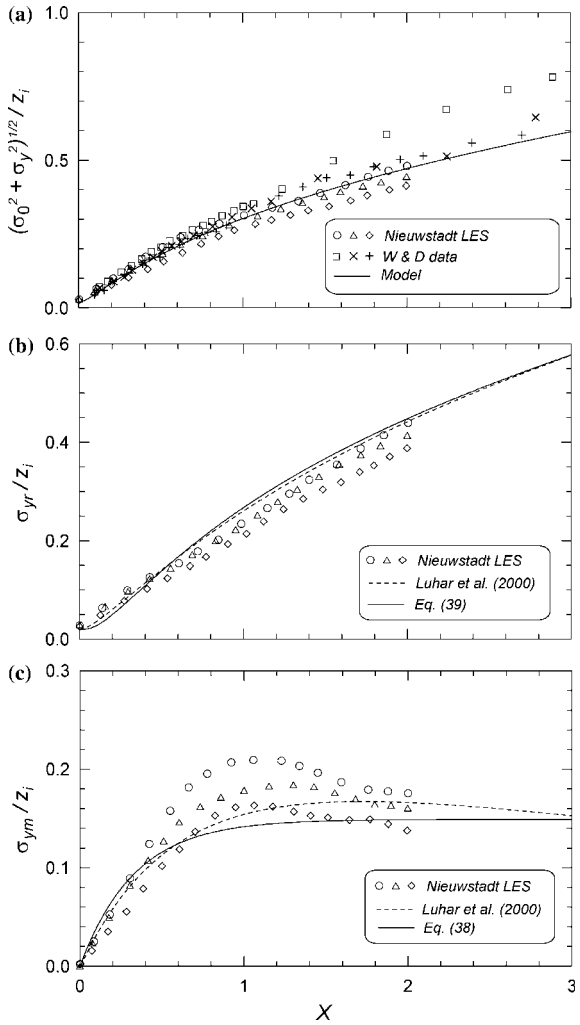

Figure 9. Variation with X of (a) the normalised total lateral spread calculated using Equation (15) (solid line), (b) the normalised lateral relative spread calculated from using Equation (39) (solid line), (c) the normalised lateral meander spread calculated using Equation (38) (solid line). The tank data of Willis and Deardorff (1976, 1978, 1981) are for the scaled source heights $z_s/z_i = 0.067$ (open squares), 0.24 (crosses), and 0.49 (pluses); The LES results of Nieuwstadt (1992) are for $z_s/z_i = 0.15$ (open circles), 0.25 (open triangles), and 0.50 (open diamonds). The dashed lines are the parameterisations of Luhar et al. (2000).

large times, the solid line levels off whereas the dashed line reaches a (wide) peak and then gradually decreases. This difference may not, however, be significant in terms of fluctuations because the total spread is dominated by relative dispersion at such times.

In the vertical direction, because the turbulence is inhomogeneous and skewed, and the plume is affected by the boundaries, the vertical meander or

relative plume spread cannot be determined explicitly, either analytically or numerically, using the present IECM model.

5. Conclusions

We have extended the use of the interaction-by-exchange-with-the-conditional-mean (IECM) mixing model to calculate concentration statistics with good results in the strongly inhomogeneous, skewed turbulence of the CBL. The model is in good agreement with laboratory convection tank data for the intensity of concentration fluctuations for both point and line sources. The point-source cumulative distribution functions predicted by the model also agree reasonably well with laboratory measurements.

The two critical aspects of the model are the conditional mean concentration and the mixing time scale. Since the horizontal and vertical velocity fluctuations are independent when neglecting the mean shear, the conditional mean concentration can be factored into the product of terms conditioned separately on each velocity component. Furthermore, since the conditional mean concentration is a one-point statistic, it is independent of micromixing and so can be pre-calculated from a one-point marked particle model. The horizontal velocity fluctuations are approximately homogeneous and Gaussian so we were able to write down an analytical expression for the term conditional on the lateral velocity. We calculated the term conditional on the vertical velocity numerically with a marked particle model for the vertical velocity in the CBL.

We followed Sawford (2004) in basing the mixing time scale on the time scale of the instantaneous plume and so modelling it as a linear function of travel time with a constant value determined by the source size for small times. For a line source, best agreement with the data was obtained with a value of 0.9 for the coefficient of the linear term, close to the value of 1.2 used by Sawford for a line source in grid turbulence. For a point source, a lower value of 0.6 gave the best agreement, reflecting the increased mixing efficiency in a two-dimensional plume.

Using these representations of the mixing time scale, we also calculated the skewness and kurtosis of the concentration field and the concentration pdf. We found that non-Gaussian features persist into the vertical well-mixed region ($X > 3$).

As shown by Sawford (2004), in the limit of vanishing mixing time scale the IECM model reduces to a meandering plume model. Thus we were able to calculate the contribution of plume meandering to the concentration fluctuation intensity in the CBL, finding that for a line source meandering is negligible for the nondimensional downwind distance $X > 1.5$ whereas for a point source that is true for about $X > 3$.

For the horizontal motions, we also were able to calculate the meandering and relative dispersion contributions to the total plume dispersion using the micromixing framework, showing that all three quantities are in excellent agreement with Luhar et al.'s (2000) model based on filtering techniques and in good overall agreement with large-eddy simulation data.

A major advantage of the micromixing approach is that it is more general than, for example, the meandering plume approach, with only the mixing time left to be specified. However, it is computationally much more intensive than the latter, but this problem could be overcome to some extent by using better sampling methods than the basic bin-counting method used in this paper. A potential extension of the micromixing approach is in the area of turbulent dispersion of chemically reactive species in the atmosphere.

In this paper, we have not carried out any quantitative analysis of possible numerical errors caused by factors such as the finite number of samples (i.e. particles), discretisation of the model equations, the number of cells used for the flow domain discretisation, and the quality of random numbers, especially in the predictions of higher-order moments of concentration (e.g. skewness and kurtosis). In our computations, the properties of these factors were selected so as to obtain a reasonable degree of smoothness and convergence of results.

Acknowledgements

The authors are thankful to Dr. Mark Hibberd for providing his water tank data, and to the two anonymous referees for their useful comments.

Appendix A: Expressions for $P_E(w,z)$, $Q_0(w,z)$ and $\phi(w,z)$

The expressions for the quantities $P_E(w,z)$, $Q_0(w,z)$ and $\phi(w,z)$ used in the model are given below (Luhar et al., 1996):

$$P_E(w,z) = A(z)P_A(w,z) + B(z)P_B(w,z), \tag{A1}$$

where

$$P_A(w,z) = \frac{1}{\sqrt{2\pi}\sigma_A}\exp\left\{-\frac{(w-\bar{w}_A)^2}{2\sigma_A^2}\right\}, \quad P_B(w,z) = \frac{1}{\sqrt{2\pi}\sigma_B}\exp\left\{-\frac{(w+\bar{w}_B)^2}{2\sigma_B^2}\right\},$$

$$\sigma_A = (\overline{w^2})^{1/2}\left\{\frac{B}{A(1+m^2)}\right\}^{1/2}, \quad \sigma_B = (\overline{w^2})^{1/2}\left\{\frac{A}{B(1+m^2)}\right\}^{1/2}, \quad B = 1-A,$$

$$A = \frac{1}{2}\left\{1-\left(\frac{r}{4+r}\right)^{1/2}\right\}, \text{ and } r = \frac{(1+m^2)^3 S_w^2}{(3+m^2)^2 m^2}.$$

$$Q_0 = \frac{A(w-\bar{w}_A)}{\sigma_A^2} P_A + \frac{B(w+\bar{w}_B)}{\sigma_B^2} P_B, \tag{A2}$$

and

$$\begin{aligned}\phi = &-\frac{1}{2}\left(A\frac{\partial \bar{w}_A}{\partial z} + \bar{w}_A \frac{\partial A}{\partial z}\right)\mathrm{erf}\left(\frac{w-\bar{w}_A}{\sqrt{2}\sigma_A}\right) \\ &+ \sigma_A\left\{A\frac{\partial \sigma_A}{\partial z}\left(\frac{w^2}{\sigma_A^2}+1\right) + \frac{Aw}{\sigma_A^2}\left(\sigma_A\frac{\partial \bar{w}_A}{\partial z} - \bar{w}_A\frac{\partial \sigma_A}{\partial z}\right) + \sigma_A\frac{\partial A}{\partial z}\right\}P_A \\ &+ \frac{1}{2}\left(B\frac{\partial \bar{w}_B}{\partial z} + \bar{w}_B \frac{\partial B}{\partial z}\right)\mathrm{erf}\left(\frac{w+\bar{w}_B}{\sqrt{2}\sigma_B}\right) \\ &+ \sigma_B\left\{B\frac{\partial \sigma_B}{\partial z}\left(\frac{w^2}{\sigma_B^2}+1\right) - \frac{Bw}{\sigma_B^2}\left(\sigma_B\frac{\partial \bar{w}_B}{\partial z} - \bar{w}_B\frac{\partial \sigma_B}{\partial z}\right) + \sigma_B\frac{\partial B}{\partial z}\right\}P_B.\end{aligned} \tag{A3}$$

Appendix B: Derivation of Concentration Conditional on Velocity

We consider the example of one-dimensional dispersion in the vertical direction. In order to calculate the conditional mean concentration due to an instantaneous area source distribution $Q_1 S(z')/U$, we consider the backward trajectories starting at the receptor location z at time t with velocity w. Then

$$\langle c; w\rangle = \frac{Q_1}{U}\int_{-\infty}^{\infty} P(z', 0; z, w, t) S(z')\, dz'. \tag{B1}$$

Neglecting streamwise diffusion, the above is equivalent to the conditional mean concentration due a continuous line source of strength Q_1.

Now, by Bayes theorem

$$\begin{aligned} P(z', 0; z, w, t) &= P(z', 0, w, t; z, t)/P(w, t; z, t), \\ &= P(z', 0, w, t; z, t)/P_{\mathrm{E}}(w; z), \\ &= P(w, t; z, t, z', 0)\cdot P(z', 0; z, t)/P_{\mathrm{E}}(w; z), \\ &= P(w, t; z, t, z', 0)\cdot P(z, t; z', 0)/P_{\mathrm{E}}(w; z), \\ &= P(z, w, t; z', 0)/P_{\mathrm{E}}(w; z), \end{aligned} \tag{B2}$$

where $P_{\mathrm{E}}(w; z)$ is the Eulerian vertical velocity pdf at height z, $P(z, w, t; z', 0)$ is the forward joint pdf of particle position and velocity at time t given the initial condition $z = z'$ at $t = 0$, and we have used the equivalence between backwards and forwards displacement probabilities,

$P(z,t;z',0) = P(z',0;z,t)$. Hence, Equation (20) follows from Equations (B1) and (B2).

We emphasise that in inhomogeneous turbulence $P(z',0;z,w,t) \neq P(z,t;z',0,w,t)$, although these pdfs are equal in homogeneous Gaussian turbulence (e.g., in the lateral direction) for which $P(w,t;z',0) = P(w,t;z,t) = P_{\mathrm{E}}(w)$.

References

Borgas, M. S. and Sawford, B. L.: 1994, 'A Family of Stochastic Models for Two-Particle Dispersion in Isotropic Homogeneous Stationary Turbulence', *J. Fluid Mech.* **289**, 69–99.

Cassiani, M. and Giostra, U.: 2002, 'A Simple and Fast Model to Compute Concentration Moments in a Convective Boundary Layer', *Atmos. Environ.* **36**, 4717–4724.

Csanady, G. T.: 1967, 'Concentration Fluctuations in Turbulent Diffusion', *J. Atmos. Sci.* **24**, 21–28.

Deardorff, J. W. and Willis, G. E.: 1984, 'Groundlevel Concentration Fluctuations from a Buoyant and a Non-Buoyant Source within a Laboratory Convectively Mixed Layer', *Atmos. Environ.* **18**, 1297–1309.

Deardorff, J. W. and Willis, G. E.: 1985, 'Further Results from a Laboratory Model of the Convective Planetary Boundary Layer', *Boundary-Layer Meteorol.* **32**, 205–236.

Fox, R. O.: 1996, 'On Velocity Conditioned Scalar Mixing in Homogeneous Turbulence', *Phys. Fluids* **8**, 2678–2691.

Fox, R. O.: 1998, 'On the Relationship between Lagrangian Micromixing Models and Computational Fluid Dynamics', *Chem. Eng. Process.* **37**, 521–535.

Franzese, P.: 2003, 'Lagrangian Stochastic Modelling of a Fluctuating Plume in the Convective Boundary Layer', *Atmos. Environ.* **37**, 1691–1701.

Franzese, P. and Borgas, M. S.: 2002, 'A Simple Relative Dispersion Model for Concentration Fluctuations in Contaminant Clouds', *J. Appl. Meteorol.* **41**, 1101–1111.

Gardiner, C. W.: 1983, *Handbook of Stochastic Methods for Physics, Chemistry, and the Natural Sciences*, Springer-Verlag, Berlin, 442 pp.

Gifford, F. A.: 1959, 'Statistical Properties of a Fluctuating Plume Dispersion Model', *Adv. Geophys.* **6**, 117–137.

Hibberd, M. F.: 2000, 'Vertical dispersion of a Passive Scalar in the Convective Boundary Layer: New Laboratory Results', in preprint, *11th AMS Conference on the Applications of Air Pollution Meteorology*, American Meteorological Society, Boston, pp. 18–23.

Luhar, A. K.: 2002, 'The Influence of Vertical Wind Direction Shear on Dispersion in the Convective Boundary Layer and its Incorporation in Coastal Fumigation Models', *Boundary-Layer Meteorol.* **102**, 1–38.

Luhar, A. K. and Britter, R. E.: 1989, 'A Random Walk Model for Dispersion in Inhomogeneous Turbulence in a Convective Boundary Layer', *Atmos. Environ.* **23**, 1911–1924.

Luhar, A. K., Hibberd, M. F., and Borgas, M. S.: 2000, 'A Skewed Meandering Plume Model for Concentration Statistics in the Convective Boundary Layer', *Atmos. Environ.* **34**, 3599–3616.

Luhar, A. K., Hibberd, M. F., and Hurley, P. J.: 1996, 'Comparison of Closure Schemes used to Specify the Velocity PDF in Lagrangian Stochastic Dispersion Models for Convective Conditions', *Atmos. Environ.* **30**, 1407–1418.

Monin, A. S. and Yaglom, A. M.: 1975, *Statistical Fluid Mechanics*, Vol. 2, MIT Press, Cambridge, MA, 874 pp.

Nieuwstadt, F. T. M.: 1992, 'A Large-Eddy Simulation of a Line Source in a Convective Atmospheric Boundary Layer – I. Dispersion Characteristics', *Atmos. Environ.* **26A**, 485–495.

Pope, S. B.: 1998, 'The Vanishing Effect of Molecular Diffusivity on Turbulent Dispersion: Implications for Turbulent Mixing and the Scalar Flux', *J. Fluid Mech.* **359**, 299–312.

Pope, S. B.: 2000, *Turbulent Flows*, Cambridge University Press, Cambridge, U.K., 806 pp.

Sawford, B. L.: 2004, 'Micro-Mixing Modelling of Scalar Fluctuations for Plumes in Homogeneous Turbulence', *Flow Turb. Combust.* **72**, 133–160.

Sawford, B. L. and Stapountzis, H.: 1986, 'Concentration Fluctuations According to Fluctuating Plume Models in One and Two Dimensions', *Boundary-Layer Meteorol.* **37**, 89–105.

Subramaniam, S. and Pope, S. B.: 1998, 'A Mixing Model for Turbulent Reactive Flows Based on Euclidean Minimum Spanning Trees', *Combustion and Flame* **115**, 487–514.

Thomson, D. J.: 1987, 'Criteria for the Selection of the Stochastic Models of Particle Trajectories in Turbulent Flows', *J. Fluid Mech.* **180**, 529–556.

Thomson, D. J.: 1997, 'Eulerian Analysis of Concentration Fluctuations in Dispersing Plumes and Puffs', *Phys. Fluids* **9**, 2349–2354.

Thomson, D. J., Physick, W. L., and Maryon, R. H.: 1997, 'Treatment of Interfaces in Random Walk Dispersion Models', *J. Appl. Meteorol.* **36**, 1284–1295.

Weil, J. C., Snyder, W. H., Lawson, Jr., R. E., and Shipman, M. S.: 2002, 'Experiments on Buoyant Plume Dispersion in a Laboratory Convection Tank', *Boundary-Layer Meteorol.* **102**, 367–414.

Willis, G. E. and Deardorff, J. W.: 1976, 'A Laboratory Model of Diffusion into the Convective Planetary Boundary Layer', *Quart. J. Roy. Meteorol. Soc.* **102**, 427–445.

Willis, G. E. and Deardorff, J. W.: 1978, 'A Laboratory Study of Dispersion from an Elevated Source within a Modeled Convective Planetary Boundary Layer', *Atmos. Environ.* **12**, 1305–1311.

Willis, G. E. and Deardorff, J. W.: 1981, 'A Laboratory Study of Dispersion from a Source in the Middle of the Convective Mixed Layer', *Atmos. Environ.* **15**, 109–117.

Yamanaka, T., Tatsuki, S., and Shimada, M. R.: 2003, 'An Individual-Based Model for Sex-Pheromone-Oriented Flight Patterns of Male Moths in a Local Area', *Ecol. Model.* **161**, 35–51.

Yee, E., Chan, R., Kosteniuk, P. R., Chandler, G. M., Biltoft, C. A., and Bowers, J. F.: 1994, 'Incorporation of Internal Fluctuations in a Meandering Plume Model of Concentration Fluctuations', *Boundary-Layer Meteorol.* **67**, 11–39.